electronics

MDPI

Article

Parametric Design of a Class of Full-Band Waveguide Differential Phase Shifters

Juan Luis Cano [1,*], Angel Mediavilla [1] and Abdelwahed Tribak [2]

[1] Department Ingeniería de Comunicaciones, Edif. Ingeniería de Telecomunicación, Universidad de Cantabria, Plaza de la Ciencia s/n, 39005 Santander, Spain; angel.mediavilla@unican.es

[2] Institut National des Postes et Telecomunications 2, Av. Allal El Fassi, 10000 Rabat, Morocco; tribak_ma@yahoo.fr

* Correspondence: juanluis.cano@unican.es; Tel.: +34-942-200919

Received: 5 March 2019; Accepted: 19 March 2019; Published: 21 March 2019

Abstract: Differential phase shifters are common circuits in communication systems where a fixed phase difference between two points within the circuit is required. Among the available technologies, waveguide phase shifters are preferred for applications such as antenna feed or beam-forming networks. Typical designs in the literature are devoted to specific phase delays such as 90° or 180°, but any phase shift might be required, and therefore a design procedure resulting in mechanically-related parameter fitting equations for any arbitrary phase difference would be advantageous. This paper presents a parametric design of full-band (40% relative bandwidth) waveguide differential phase shifters, providing polynomial equations for all design parameters in order to obtain arbitrary phase shifts between standard rectangular waveguides with equal physical lengths. The phase shift is achieved through the use of a multi-step ridge section together with a single width-step in the shift line. The proposed design procedure results in differential phase shifters with 25 dB of return loss and minimal physical length for any phase shift between 0° and 180°. To validate this parametric design process, two exemplary differential phase shifters with 30° and 140° phase shifts were measured, showing very good agreement with the simulated results.

Keywords: differential phase shifter; full-band; ridge; waveguide

1. Introduction

Differential phase shifters (DPSs) are common components in many applications where a fixed phase difference is required between two points within a circuit. The applications include phase discriminators, beam forming networks, power dividers and phase array antennas. Typically, 90° or 180° DPSs are needed in most communication systems but, in general, any phase difference may be required for a specific application and therefore DPSs with arbitrary phase shifts and stringent performances are still of importance for microwave designers. Moreover, a parametric design procedure that enables one to obtain a full-band and high return loss DPS with minimum insertion loss for any phase difference, with respect to a reference line with the same physical length, is of great interest and provides improved flexibility in waveguide system architectures.

Many different technologies have been developed through the years for obtaining a differential phase shift within a circuit. This work deals with ridge waveguide-based DPSs because the structures based on planar circuits, such as microstrip technology [1], despite having a compact size, exhibit noticeable insertion loss and low power handling capabilities that hinder their utilization in many antenna feed networks. Substrate integrated waveguide (SIW) technology has emerged as an option for combining advantages from planar technology, such as compactness and low cost, and waveguide technology, such as high quality factors and low insertion loss. Different DPS structures have been

proposed in SIW technology in recent years [2,3] that attempt to conjugate all these advantages. However, hollow waveguide technology remains the best option for feed networks where the electrical requirements in terms of insertion loss, power handling capabilities, performance repeatability and mechanical rigidity, are of utmost importance. Achievement of the desired phase difference in a waveguide is generally obtained through variation of the waveguide propagation constant in the shift line. One way to do this is to modify the dielectric constant with the introduction of dielectric slabs [4] or ferrite materials [5,6]. These structures can be easily designed to get any arbitrary phase shift, but their insertion loss is increased with the dielectric constant accordingly. An alternative procedure to change the propagation constant is to vary the waveguide physical dimension. Thus, in [7], the inclusion of a series of E-plane stubs enables one to obtain a DPS with excellent phase performance in a 17% bandwidth. Unfortunately, this configuration requires a reference line with a different physical length, which may affect the circuit symmetry and integration. The use of waveguide corrugations [8–10] has demonstrated good electrical results in designs with up to 30–35% bandwidth. The combination of high return loss, small shift errors and large bandwidths in these structures requires a large number of corrugations, thus affecting the compactness and easy-machining concepts. Finally, metallic ridges synthetized with fins or pins following stepped or continuous profiles have emerged as the best solution for their electrical performance [10–13]. However, among these last DPSs, those implemented with pins or smoothed profiles are more challenging during their design stages and show a noticeable increase in mechanical complexity, resulting in higher costs. In a previous work [14], a ridge-based DPS was presented with full-band (40%) coverage in Ku-band and 25 dB of return loss showing $\pm 2.5^\circ$ and $\pm 3.5^\circ$ shift errors for a 90°-DPS and 180°-DPS respectively. Although this structure, as presented in [14], can be easily scaled to other frequency bands, it cannot be straightforwardly modified to meet other phase difference values unless the design process is restarted. Therefore, a parametric design that provides fitting equations for any desired phase shift is of great interest for DPS designers.

Focusing on the concepts of minimum physical length and the same number of matching steps for all phase difference values, in this paper we present a parametric study of a ridge-based differential phase shifter resulting in fitting equations that enable a fast and accurate design process for obtaining a DPS with any arbitrary phase difference between the shift and reference lines with equal physical lengths. Furthermore, the electrical performance exhibits full-band coverage (40% relative bandwidth) with, at least, 25-dB return loss and minimum insertion loss. All these characteristics are combined with an easy mechanization that facilitates frequency scaling and provides robustness against mechanical tolerances.

Section 2 details the design of a generic differential phase shifter providing suitable fitting equations and parameter values for all phase differences. Experimental validation of the two exemplary DPSs is given in Section 3. Finally, Section 4 presents some conclusions.

2. Differential Phase Shifter Design

The ridge waveguide differential phase shifter used in the current parametric study follows the previously presented configuration in [14], which is shown in Figure 1 together with its reference line, an empty standard rectangular waveguide. As it is generally known, a ridge waveguide exhibits a wider mono-mode bandwidth than its empty waveguide counterpart due to the reduction of the fundamental mode cutoff frequency [15]. On the other hand, the operational bandwidth of a DPS is commonly defined based on the acceptable phase shift deviation with respect to the desired phase difference. Depending on this shift accuracy, a DPS with the same electrical performance may show different bandwidths. Corrugation-based DPSs [8–10] exhibit a quadratic-like phase difference curve that rapidly deviates from the desired phase value; however, ridge-based DPSs show a cubic-like curve, which widens the frequency range with controlled phase error. This feature, together with the aforementioned increased mono-mode bandwidth, clearly points at ridge DPS as the best solution for waveguide wideband applications.

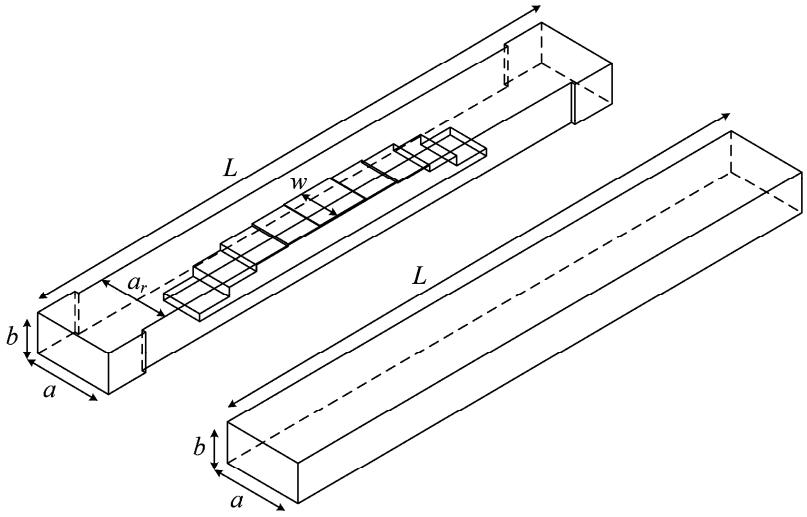

Figure 1. 3D sketch of the generic ridge waveguide differential phase shifter: shift and reference waveguides.

Before starting the design process for a frequency range (40% relative bandwidth) defined by its lowest and upper frequencies (f_1 and f_2 respectively), some constraints have to be imposed on the structure, otherwise multiple sets of parameter values could be obtained for a determined electrical response, thus affecting the systematicity of this study. Firstly, in this work, the ridge thickness, w in Figure 1, has been fixed to the waveguide height value b, $w = b$. Alternative and valid parameter values could be found, starting with another ridge thickness value. Secondly, the number of ridge matching steps has been set to $n = 4$, whatever the phase difference desired value is. These matching steps perform two functions: on one side they introduce part of the final phase shift, and on the other side they act as impedance transformers that provide the DPS matching. The larger the number of matching steps the higher the return loss, at the expense of higher design and mechanization complexities. Finally, since the phase delay is a periodic function, the same phase shift can be achieved with different physical lengths, so therefore the design process is followed upon the premise of the minimum physical length of the DPS.

A simplified scheme of the DPS is shown in Figure 2 together with the relevant physical and electrical parameters that are required for understanding the subsequent equations. The shift line is composed of two symmetric networks, each one made up of an initial empty section with dimensions a_r, b and length L_G which is followed by $n = 4$ matching steps, with dimensions h_i and l_{si}, $i = 1 \ldots n$, and finally, a ridge section with dimensions h_r and $l_r/2$. This structure is directly connected with the standard waveguide of dimensions a and b. The width step between a and a_r is introduced to match the fundamental mode cutoff frequency between the empty and ridge waveguides.

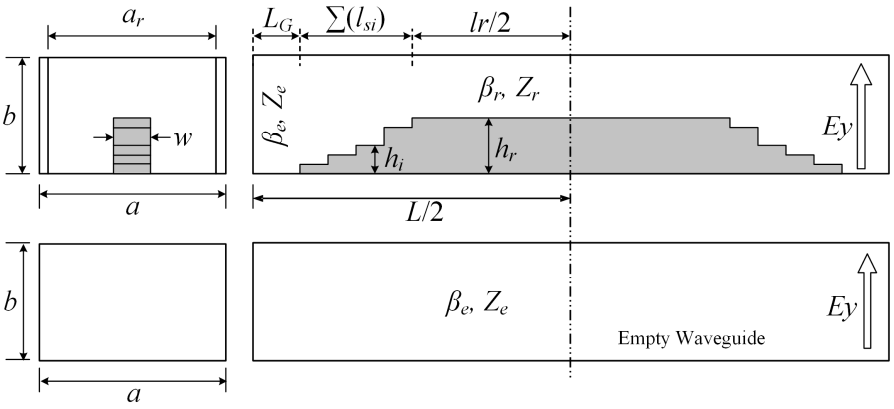

Figure 2. Scheme of the DPS with physical and electrical parameters definition.

The previous scheme is modeled with an equivalent mono-mode circuit as shown in Figure 3 (only one half). In this model, each step discontinuity corresponds to a shunt susceptance whose value is obtained from the generalized scattering matrix associated to this discontinuity by using the modal scattering analysis developed in [11], and by extracting the values corresponding to the fundamental mode from the generalized scattering matrix. Additionally, rectangular and ridged waveguide sections can be modeled in the mono-mode approach by a simple dispersive transmission line where the characteristic admittances and propagation constants can be calculated from [15]. In Figure 3, the different step susceptances, B_{si}, propagation constants, β_{si} and β_r, and waveguide impedances, Z_{si} and Z_r, are the geometry-related design parameters with respect to an empty waveguide of the same length L defined by β_e and Z_e.

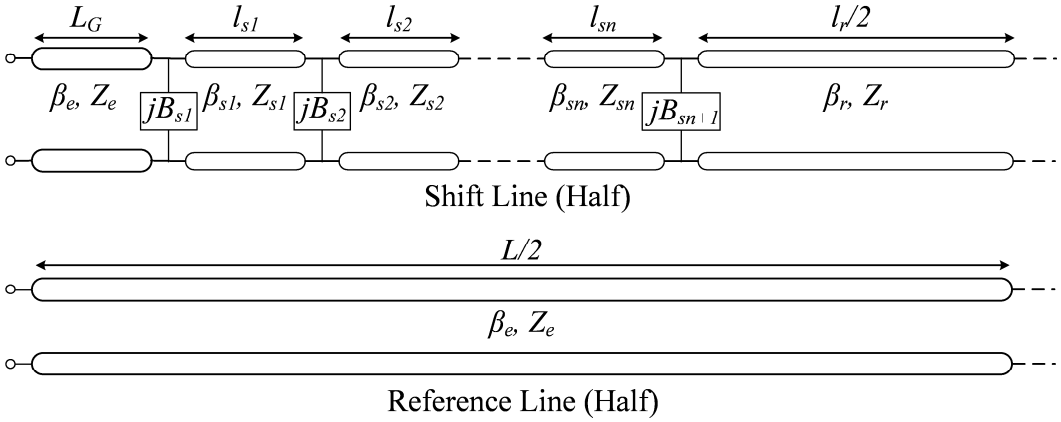

Figure 3. Mono-mode electrical equivalent circuit for one half DPS.

With the parameters defined in Figure 3, the ABCD matrix of half DPS can be established (1), and using this matrix it is feasible to obtain the overall input impedance (2) and voltage transfer ratio (3). From this last expression, the amplitude must be equal to the unity and the phase must be equal to the nominal phase shift value with respect to the reference waveguide, i.e., the desired phase difference between both waveguides. Once the different parameters have been calculated, these values are translated back to physical dimensions by using the mono-mode generalized scattering matrix method. Performing this procedure for selected phase difference values within the total range of possible phase shifts allows fitting curves for the physical parameters to be extracted in order to get useful tools that help in the design of DPSs with arbitrary phase shifts.

$$\begin{pmatrix} A_h & B_h \\ C_h & D_h \end{pmatrix} = \begin{pmatrix} \cos\theta_e & jZ_e\sin\theta_e \\ jY_e\sin\theta_e & \cos\theta_e \end{pmatrix} \begin{pmatrix} 1 & 0 \\ jB_{s1} & 1 \end{pmatrix} \begin{pmatrix} \cos\theta_{s1} & jZ_{s1}\sin\theta_{s1} \\ jY_{s1}\sin\theta_{s1} & \cos\theta_{s1} \end{pmatrix} \cdot \begin{pmatrix} 1 & 0 \\ jB_{s2} & 1 \end{pmatrix} \cdots \begin{pmatrix} 1 & 0 \\ jB_{sn} & 1 \end{pmatrix} \begin{pmatrix} \cos(\theta_r/2) & jZ_r\sin(\theta_r/2) \\ jY_r\sin(\theta_r/2) & \cos(\theta_r/2) \end{pmatrix} \tag{1}$$

$$Z_{in} = \frac{Z_e \cdot (A_h \cdot D_h - B_h \cdot C_h) + 2 \cdot A_h \cdot B_h}{(A_h \cdot D_h + B_h \cdot C_h) + 2 \cdot C_h \cdot D_h \cdot Z_e} \tag{2}$$

$$\Delta V = \frac{Z_e \cdot (A_h \cdot D_h - B_h \cdot C_h) + 2 \cdot A_h \cdot B_h}{Z_e \cdot (A_h \cdot D_h + B_h \cdot C_h)} \tag{3}$$

In order to perform a parametric study, in this work we calculated physical dimension values for phase shifts from 20° to 180° in 10° steps. Then, these values were fitted with 3rd-order polynomial equations as presented in (4), obtaining a fitting error of less than 2%. Coefficients of the fitting polynomials are given in Table 1, where widths and heights are normalized to the standard waveguide dimensions a and b, respectively, and the lengths are normalized to λ_g, where λ_g is the empty waveguide wavelength at the center frequency, $f_0 = (f_1 \times f_2)^{1/2}$. Finally, the design parameters

obtained from these equations are used as an initial guess for the mode-matching simulation tool μWave-Wizard from Mician GmbH. Minor optimization of the geometric dimensions in this tool is sufficient to meet the required specifications. The optimization process follows these guidelines: the desired bandwidth is firstly set, always aiming at a 40% relative bandwidth, and then all the mechanical dimensions are optimized trying to meet two main goals. These two goals are a return loss of 25 dB or better and achievement of the nominal phase shift with minimum phase error. Obviously, for each phase shift nominal value the phase error is different, increasing as the corresponding nominal value does.

$$p = a_3 \cdot d^3 + a_2 \cdot d^2 + a_1 \cdot d + a_0 \tag{4}$$

In (4), parameter p stands for any DPS physical dimension as given in Table 1 and d is the desired broadband phase delay in degrees. Curves for all design parameters are plotted in Figure 4.

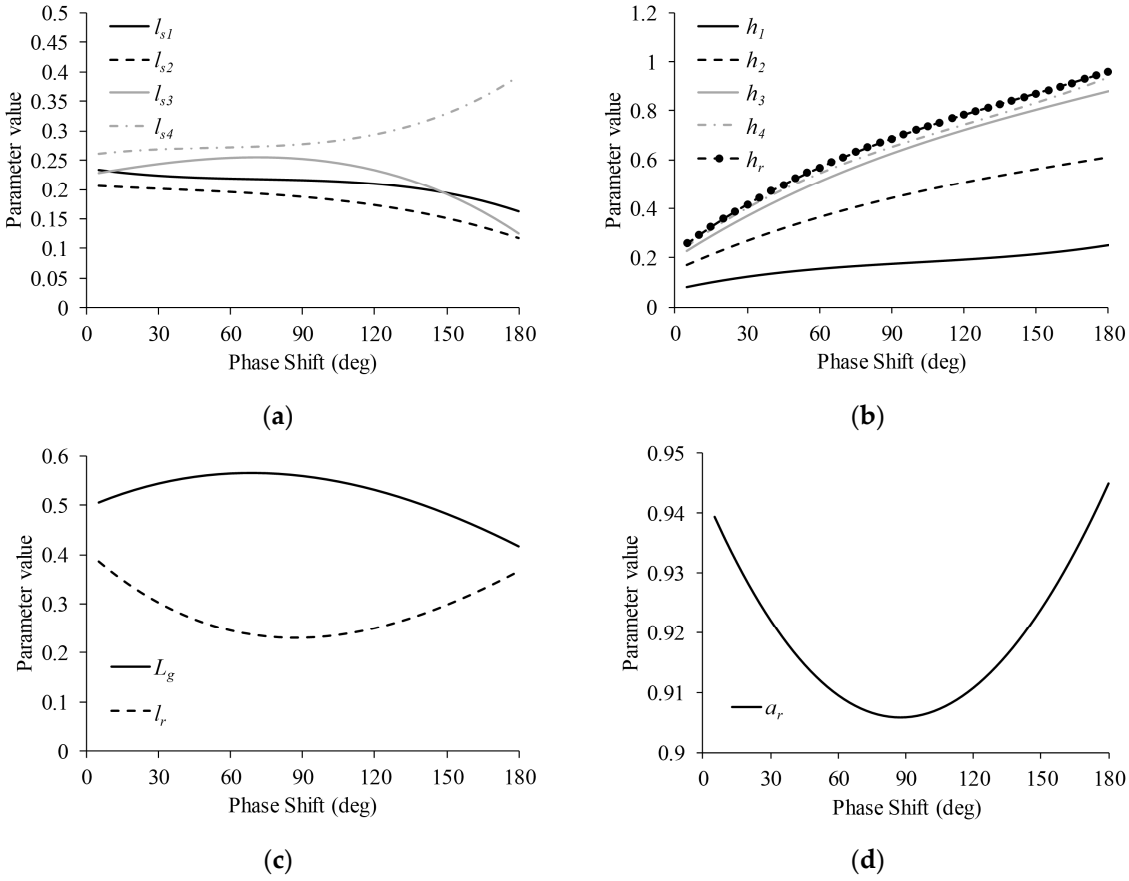

Figure 4. Parameter values: (**a**) matching step lengths normalized to λ_g; (**b**) matching step and ridge heights normalized to b; (**c**) input empty section and central ridge lengths normalized to λ_g; (**d**) ridge waveguide width normalized to a.

Table 1. Coefficients for the fitting equations of the DPS's parameters. Widths and heights are normalized to the standard waveguide dimensions a and b respectively; lengths are normalized to λ_g, where λ_g is the empty waveguide wavelength at the center frequency.

Parameter	a_3 ($\times 10^{-8}$)	a_2 ($\times 10^{-5}$)	a_1 ($\times 10^{-3}$)	a_0 ($\times 10^{-1}$)
a_r	−0.1957	0.5278	−0.8793	9.4366
L_G	1.6409	−1.7033	2.1022	4.9358
l_r	−4.2373	3.0740	−4.3881	4.0689
h_r	7.0981	−3.0946	7.3638	2.2122
l_{s1}	−3.5746	0.7551	−0.6181	2.3556
l_{s2}	−1.8315	0.1853	−0.2390	2.0784
l_{s3}	−2.7420	−0.2120	0.7188	2.2440
l_{s4}	5.3796	−0.8540	0.5432	2.5766
h_1	5.2236	−1.5878	2.1594	0.7088
h_2	2.7859	−1.5288	4.4140	1.5010
h_3	3.7330	−2.0775	6.3168	1.9579
h_4	9.6739	−3.5746	7.3091	2.1230

Following the previous equations, different DPSs for phase delays from 20° to 180° in 10° steps were designed in the 10–15 GHz frequency band. The corresponding electrical performances are presented in Figure 5. As can be appreciated, all the designed DPSs have a return loss of 25 dB, whereas the phase errors range from ±0.5° for the 20°-DPS to ±3.1° for the 180°-DPS.

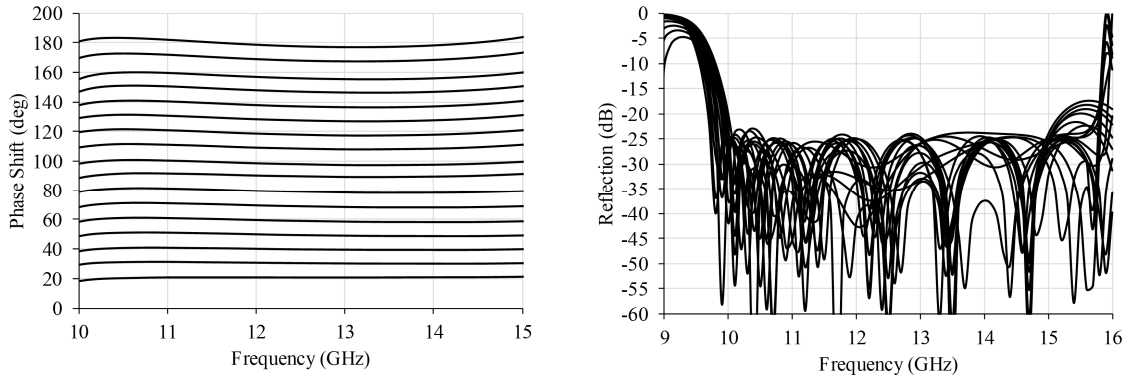

(**a**) (**b**)

Figure 5. Simulated electrical performance of the designed DPSs: (**a**) phase shift and (**b**) return loss.

3. Experimental Verification

In order to experimentally validate the parametric design detailed in the previous section, two exemplary DPSs were designed and mechanized. From the available phase shift range, we selected the 30° and 140° units to provide two alternative configurations different from the classical 90°-DPS appearing in most published works. Notwithstanding the selected units, similar results could have been found with any other phase shift election as is demonstrated in Figure 5. Final dimensions are given in Table 2.

Table 2. Final mechanical dimensions of the manufactured 30° and 140° DPSs (units in mm.).

Phase Shift	a_r	L_G	l_r	h_r	h_1	h_2	h_3	h_4	l_{s1}	l_{s2}	l_{s3}	l_{s4}
30°	17.52	16.73	9.8	4	1.22	2.62	3.54	3.83	6.85	6.23	7.42	8.32
140°	17.49	15.17	8.72	7.92	2	5.31	7.4	7.49	6.18	4.89	6.32	9.82

The DPSs were mechanized in two blocks of brass which are joined by the E-plane as shown in Figure 6. Thus, insertion loss is minimized and rounds are avoided in the waveguide inner corners. The ridge is mechanized separately and then screwed on to the corresponding waveguide inner wall. This procedure, apart from facilitating its manufacture, enables one to implement small modifications to the ridge if necessary, and therefore to the DPS tuning.

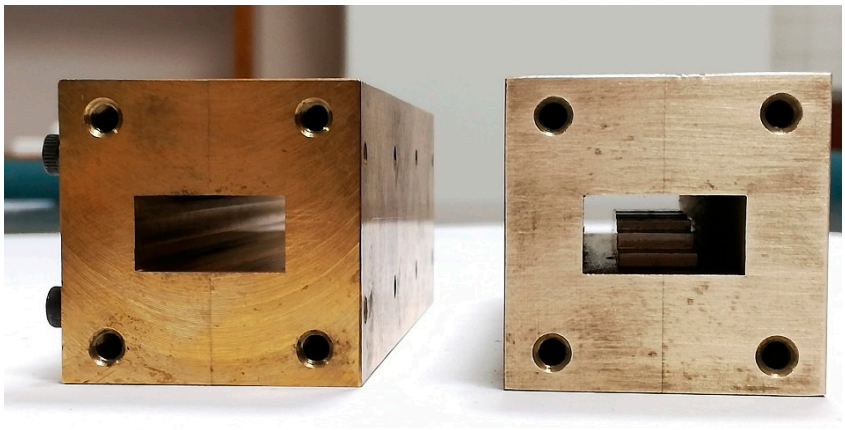

Figure 6. Photograph of one of the manufactured DPSs: reference waveguide (**left**) and shift waveguide (**right**).

For the measurement, commercial coaxial-to-WR75 transitions are connected to the vector network analyzer (VNA) and the thru-reflect-line (TRL) calibration technique is applied at the WR75 ports. Therefore, the calibration plane is established at the DPSs ports and their performance is directly measured. For the phase shift measurement, the shift and reference lines are measured and the difference between the phases of their corresponding transmission coefficients is calculated. The obtained values are presented in Figure 7 together with the simulated results for better comparison.

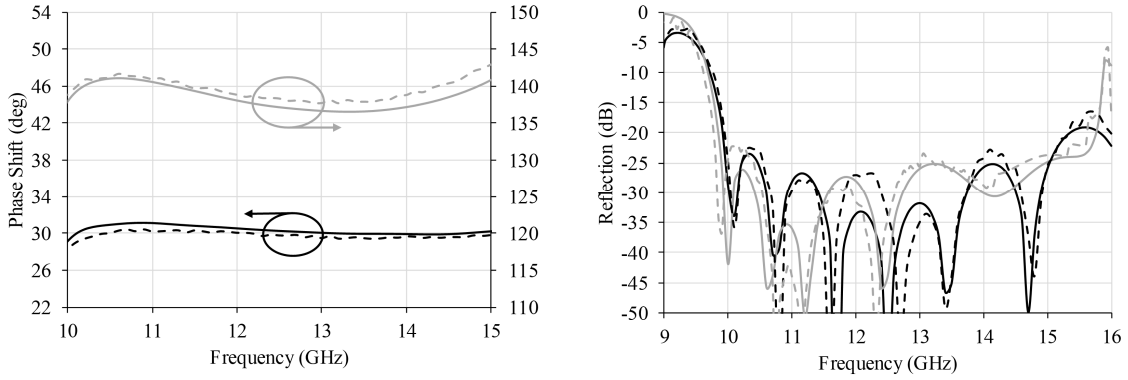

(**a**) (**b**)

Figure 7. Comparison between simulated (solid lines) and measured results (dashed lines) for the designed 30°-DPS (black lines) and 140°-DPS (grey lines): (**a**) phase difference and (**b**) reflection.

From plots in Figure 7, a good agreement between simulation and theory can be appreciated, which validates the design procedure and the obtained fitting equations. Phase shift error is ±0.6° for the 30°-DPS and ±2.5° for the 140°-DPS, whereas the return loss is around 25 dB for both circuits in the 10–15 GHz frequency range. Small differences between simulated and measured results are attributed to mechanical tolerances.

Finally, results obtained in this work are compared in Table 3 with other published waveguide DPSs following similar or alternative topologies in order to demonstrate its suitability. From these

results, the advantage of ridge DPSs over corrugated DPSs is clear. Although these last structures are from square waveguide polarizers, corresponding DPSs could have been designed in rectangular waveguides. However, the length of these structures is noticeably greater than the ridge counterparts. On the other hand, stub loaded shifters tend to be shorter in length but in this case the shift line and its reference line are of different lengths, which produces symmetry issues during integration. Finally, ridge-based DPSs made with pins or smoothed-ridge profiles increase the mechanical complexity. The former show very limited electrical performance, whereas the latter achieve a very compact design at the expense of increasing the insertion loss. Differential phase shifters based on ferrites or dielectric slabs are omitted in Table 3 due to its high losses.

Table 3. Comparison between published results of waveguide DPSs.

Ref.	BW (%) Freq. (GHz)	Return Loss (dB)	Phase Error (deg)	Insertion Loss (dB)	Length (λ_g)	Mechanical Complexity	Type
[7]	17% (10.7–12.7)	30	+2.5/−1	0.1	1	Low	Stub loaded
[8]	30% (85–115)	17	±3	0.2	3.64	Low	Corrugated
[9]	17% (35–50)	17	±6	0.1	4.6	Low	Corrugated
[12]	26% (46–60)	10	±20	<1	-	Medium/High	Ridge/Pin
[13]	40% (33–50)	20	+4/−0.5 (90°)	0.4	0.9	Medium	Ridge/Smooth
This work	40% (10–15)	25	±2.5 (140°) ±0.6 (30°)	<0.1	2.8 (140°) 2.9 (30°)	Low	Ridge

4. Conclusions

The parametric design of full-band waveguide differential phase shifters with arbitrary phase shifts, excellent return loss and compact size is presented. This parametric design process results in 3rd-order polynomial equations for all the design parameters, which enables fast and accurate calculation of physical dimensions for any phase shift value and frequency band. Both the reference line and the shift line are of the same physical length, which facilitates the DPS integration in any microwave network. Two exemplary DPSs were mechanized and measured for demonstration purposes showing around 25 dB of return loss in the 10–15 GHz band (40% relative bandwidth) and phase errors of ±0.6° for the 30°-DPS and ±2.5° for the 140°-DPS.

Author Contributions: Conceptualization, J.L.C., A.M., A.T.; Funding acquisition, A.M.; Investigation, J.L.C., A.M., A.T.; Supervision, A.M.; Validation, J.L.C.; Writing—original draft, J.L.C.; Writing—review & editing, J.L.C., A.M., A.T.

Funding: This research was supported by the State Research Agency, Spanish Ministry of Economy, Industry and Competitiveness, through project TEC2017-83343-C4-1-R and FEDER funds from the EU.

Conflicts of Interest: The authors declare no conflict of interest. The funders had no role in the design of the study; in the collection, analyses, or interpretation of data; in the writing of the manuscript, or in the decision to publish the results.

References

1. Villa, E.; Cagigas, J.; Aja, B.; de la Fuente, L.; Artal, E. Q-band 4-state phase shifter in planar technology: Circuit design and performance analysis. *Rev. Sci. Instrum.* **2016**, *87*, 094705-1–094705-9. [CrossRef] [PubMed]
2. Parment, F.; Ghiotto, A.; Vuong, T.-P.; Duchamp, J.-M.; Wu, K. Double Dielectric Slab-Loaded Air-Filled SIW Phase Shifters for High-Performance Millimeter-Wave Integration. *IEEE Trans. Microw. Theory Technol.* **2016**, *64*, 2833–2842. [CrossRef]

3. Malik, B.T.; Doychinov, V.; Robertson, I.D. Compact Broadband Electronically Controllable SIW Phase Shifter for 5G Phased Array Antennas. In Proceedings of the 12th European Conference Antennas and Propagation (EuCAP), London, UK, 9–13 April 2018; pp. 1–4.
4. Arndt, F.; Bornemann, J.; Vahldieck, R. Design of Multisection Impedance-Matched Dielectric-Slab Filled Waveguide Phase Shifters. *IEEE Trans. Microw. Theory Technol.* **1984**, *32*, 34–39. [CrossRef]
5. El-Sharawy, E.-B.; Koza, C.J. Dual-Ferrite Slot Line for Broadband, High-Nonreciprocity Phase Shifters. *IEEE Trans. Microw. Theory Technol.* **1991**, *39*, 2204–2210. [CrossRef]
6. Abdelaal, M.A.; Shams, S.I.; Kishk, A.A. Rectangular Waveguide Differential Phase Shifter Based on Horizontal Ferrite Tiles: Accurate Model for Full-Band Operation. *IEEE Access* **2019**, *7*, 23766–23778. [CrossRef]
7. Dittloff, J.; Arndt, F. Optimum Design of Waveguide E-plane Stub-Loaded Phase Shifters. *IEEE Trans. Microw. Theory Technol.* **1988**, *36*, 582–587. [CrossRef]
8. Chung, M.-H.; Je, D.-H.; Han, S.-T.; Kim, S.-R. Development of a 85~115 GHz 90-deg Phase Shifter using Corrugated Square Waveguide. In Proceedings of the 44th European Microwave Conference, Rome, Italy, 6–9 October 2014; pp. 1146–1149.
9. Zhong, W.; Yin, X.; Shi, J.; Liu, C. A Differential Waveguide Phase Shifter for Q-band Cryogenic Receivers. In Proceedings of the 6th Asia-Pacific Conference Antennas and Propagation (APCAP), Xi'an, China, 16–19 October 2017.
10. Mediavilla, A.; Pereda, J.A.; González, O.; Casanueva, A.; Helszajn, J.; Levy, R. Differential Phase Shifters Using Corrugated, Ridge, and Fin Loaded Waveguides. *Int. J. RF Microw. CAE* **2009**, *19*, 561–567. [CrossRef]
11. Bornemann, J.; Arndt, F. Modal-S-Matrix Design of Optimum Stepped Ridged and Finned Waveguide Transformers. *IEEE Trans. Microw. Theory Technol.* **1987**, *35*, 561–567. [CrossRef]
12. Palomares-Caballero, A.; Alex-Amor, A.; Padilla, P.; Luna, F.; Valenzuela-Valdes, J. Compact and Low-Loss V-band Waveguide Phase Shifter Based on Glide-Symmetric Pin Configuration. *IEEE Access* **2019**. accepted for publication. [CrossRef]
13. Villa, E.; Aja, B.; Cagigas, J.; Artal, E.; de la Fuente, L. Four-State Full Q-Band Phase Shifter Using Smooth-Ridged Waveguides. *IEEE Microw. Wirel. Comput. Lett.* **2017**, *27*, 995–997. [CrossRef]
14. Tribak, A.; Mediavilla, A.; Zbitou, J.; Cano, J.L. Novel Ridged Waveguide Differential Phase Shifter for Satellite Application. *Int. J. Microw. Opt. Technol.* **2014**, *9*, 409–414.
15. Hoefer, W.J.R.; Burton, M.N. Closed-Form Expressions for the Parameters of Finned and Ridged Waveguides. *IEEE Trans. Microw. Theory Technol.* **1982**, *30*, 2190–2194. [CrossRef]